Free vibration of double-cracked uniform beam

Aleksandar Nikolić*
Faculty of Mechanical and Civil Engineering in Kraljevo, University of Kragujevac

This paper considers free vibration analysis of double-cracked uniform beam under various boundary conditions. It is supposed that cracks stay opened due to vibrations. The Euler-Bernoulli beam model was considered by using the rigid segment method. Satisfactory agreement of the obtained results with the results of other was achieved. In the case of occurrence of larger errors, it was noticed that there is a problem of closing the crack, which deviates from the initial assumption.

Keywords: Double-cracked beam, Free vibration, Uniform beam

1. INTRODUCTION

The appearance of cracks leads to a change in the dynamic characteristics of the beam. More precisely, with the appearance of a crack, the stiffness of the beam decreases, which leads to decreasing of natural frequencies of free beam vibrations. The literature dealing with this topic is rich, so its review will not be given here.

This paper is based on the previous research of the author that is published the paper [1], where the rigid segment method was used for free vibration analysis of uniform beam with one open crack under the various boundary conditions.

Here, the usage of the rigid segment method is extended to the double-cracked beam. The position of the cracks and their depths differ from each other in a general case. The case of the free-free beam will be analysed first. All other beam boundary conditions will be provided as a special case of free-free beam.

2. APPROXIMATE MODEL OF DOUBLE-CRACKED BEAM

Figure 1(a) shows the double-cracked uniform beam that is analysed in this paper. The beam cross-section is rectangular with dimensions $b \times h$. The total beam length is L, whereas two open cracks of depth a_1 and a_2 are placed at the distances L_1 and L_2, respectively, measured from the left end of the beam.

In the first step of modelling, the cracked beam was divided into the three beams (I, II and III) of the following lengths:

$$L_I = L_1,\ L_{II} = L_2 - L_1,\ L_{III} = L - L_2. \tag{1}$$

The first and the second beam (I and II), as well as the second and the third beam (II and III) are connected mutually by the crack elastic joints J_{c_1} and J_{c_2}, respectively, as shown in Fig. 1(b).

In the second step of modelling, each of three introduced beams was divided into the n_I, n_{II} and n_{III} elastic segments, respectively, whereas this numbers are chosen by using the following formula:

$$n_i = \frac{L_i}{L} n,\ \left(i = I, II, III\right). \tag{2}$$

The number n represents the total number of elastic segments in all of the three introduced beams. The number n should be chosen so that each of numbers n_i must be an integer.

The third modeling step involves replacing each of the introduced elastic segments with two rigid segments, interconnected by joint element J_i with three degrees of freedom, as shown in Figs. 1(c) and (d).

The joint element J_i has three degrees of freedom: axial, translational and rotational. An appropriate springs are placed in the directions of the introduced degrees of freedom. The rigidity of introduced springs is defined as [1]:

$$k_{p_i} = n\frac{AE}{L},\ k_{q_i} = n\frac{EI_z}{L},\ k_{r_i} = n^3\frac{12EI_z}{L^3}, \tag{3}$$

for all values of i except for i=n_1+1 or i=n_1+n_2+2, for which, based on the references [2,3] holds that:

$$k_{p_i} = \frac{Eb}{\left(1-\nu^2\right)F_{1,j}},\ k_{q_i} = \frac{Eb}{\left(1-\nu^2\right)F_{2,j}},$$
$$k_{r_i} = \frac{Eb}{\left(1-\nu^2\right)F_{3,j}}, \tag{4}$$

where:

$$F_{k,j} = e^{\frac{1}{1-\xi_j}}\sum_{i=1}^{10} a_{k,i}\xi_j^i,\ \xi_j = a_j / h,$$
$$j = \begin{cases} 1, & i = n_1 + 1, \\ 2, & i = n_1 + n_2 + 2. \end{cases} \tag{5}$$

Note that the parameters $a_{k,i}$ are listed in the Table 1.

2.1 Kinetic energy

Kinetic energy of the approximate model of the double-cracked uniform beam model should be obtained as the positive definite quadratic form [1]:

$$T = \frac{1}{2}\dot{\mathbf{v}}^T \mathbf{M}\dot{\mathbf{v}}, \tag{6}$$

where:

*Corresponding author: Aleksandar Nikolić, Dositejeva 19, Kraljevo, nikolic.a@mfkv.kg.ac.rs

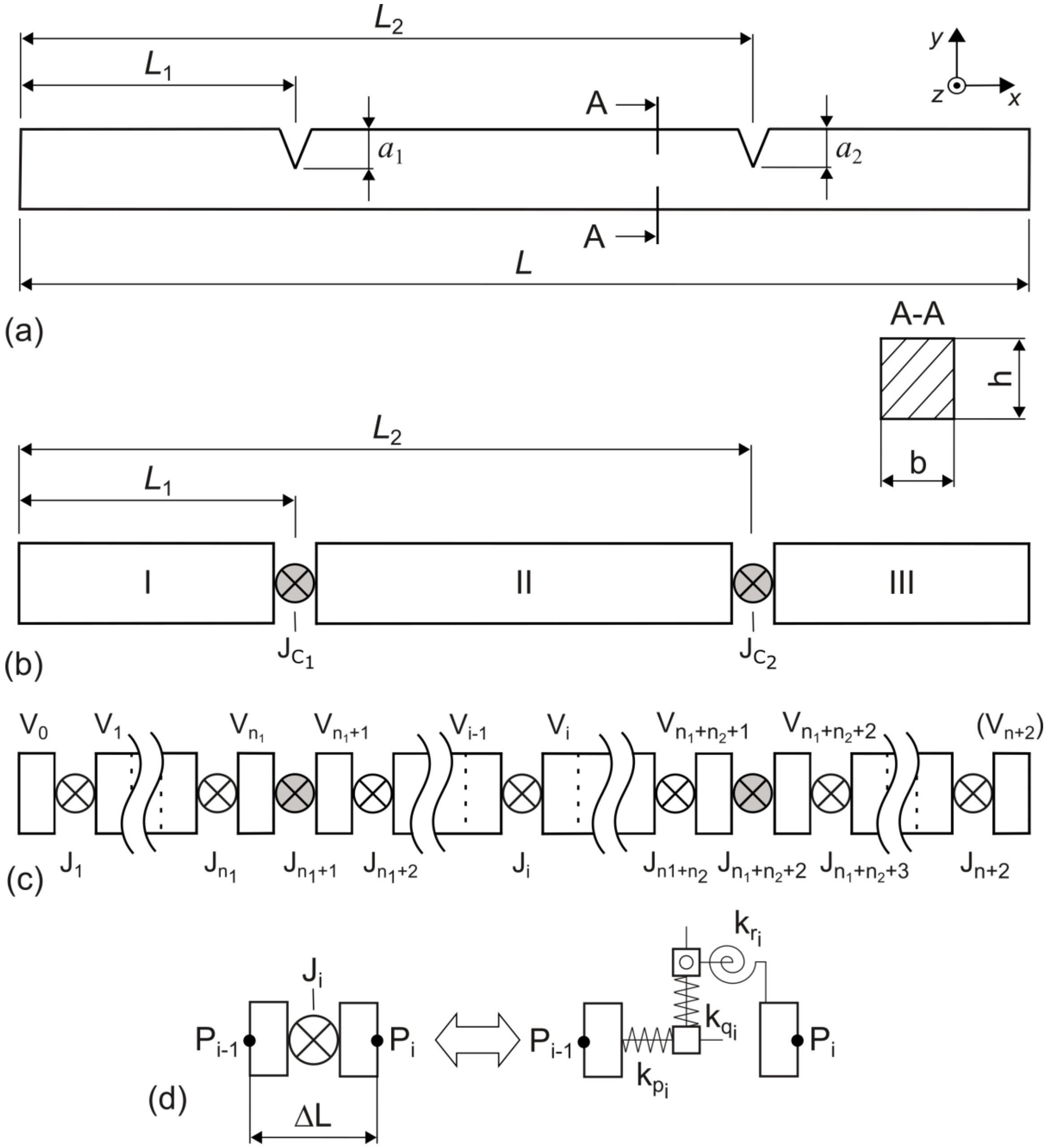

Figure 1 : Double-cracked uniform beam: (a) exact shape, (b) equivalent beam model, (c) rigid segment beam model, (d) joint element J_i

$$\dot{\mathbf{v}} = \left[\dot{\mathbf{v}}_0^T \quad \dots \quad \dot{\mathbf{v}}_i^T \quad \dots \quad \dot{\mathbf{v}}_{n+2}^T \right]^T \in R^{3(n+3)\times 1}, \tag{7}$$

$$\mathbf{M} = diag\left(\mathbf{M}_0, \dots, \mathbf{M}_i, \dots, \mathbf{M}_{n+2}\right) \in R^{3(n+3)\times 3(n+3)}, \tag{8}$$

$$\mathbf{M}_i = \left[m_{jk,i} \right] \in R^{3\times 3}, \tag{9}$$

$$\begin{aligned}
m_{11,i} &= m_{22,i} = m_i, \\
m_{33,i} &= J_{C_i\zeta_i} + m_i\left(\overline{P_iC}_{i,\xi_i}^{\;2} + \overline{P_iC}_{i,\eta_i}^{\;2}\right), \\
m_{12,i} &= m_{21,i} = 0, \\
m_{13,i} &= m_{31,i} = -m_i\overline{P_iC}_{i,\eta_i}, \\
m_{23,i} &= m_{32,i} = m_i\overline{P_iC}_{i,\xi_i},
\end{aligned} \tag{10}$$

$$m_i = \rho A l_i,\; J_{C_i\zeta_i} = \frac{1}{12} m_i l_i^2, \tag{11}$$

$$l_i = \begin{cases} \dfrac{1}{2}\dfrac{L}{n}, & i = k, \\ \dfrac{L}{n}, & i \neq k. \end{cases}$$

$$k = n_1 \vee n_1 + 1 \vee n_1 + n_2 + 1 \vee n_1 + n_2 + 2 \vee n + 2, \tag{12}$$

$$\overrightarrow{P_iC_i} = \begin{cases} \left[l_i/2 \quad 0 \quad 0\right]^T, & i = 0 \vee n_1+1 \vee n_1+n_2+2, \\ \left[-l_i/2 \quad 0 \quad 0\right]^T, & i = n_1 \vee n_1+n_2+1 \vee n+2, \\ \left[0 \quad 0 \quad 0\right]^T, & i \neq k. \end{cases} \quad (13)$$

Table 1: Coefficients $a_{k,i}$ of functions F_k

k \ i	1	2	3
1	$-0.326584\cdot10^{-5}$	$-0.326018\cdot10^{-6}$	$-0.219628\cdot10^{-4}$
2	1.455190	1.454954	52.37903
3	-0.984690	-1.455784	-130.2483
4	4.895396	-0.421981	308.442769
5	-6.501832	-0.279522	-602.445544
6	12.792091	0.455399	939.044538
7	-26.723556	-2.432830	-1310.95029
8	35.073593	5.427219	1406.52368
9	-34.954632	-6.643057	1067.4998
10	9.054062	4.466758	391.536356

2.2 Potential energy

Potential energy of the approximate model of the double-cracked uniform beam model should be obtained as the positive definite quadratic form [1]:

$$\Pi = \frac{1}{2}\mathbf{v}^T\mathbf{K}\mathbf{v}, \quad (14)$$

where:

$$\mathbf{v} = \left[\mathbf{v}_0^T \quad \cdots \quad \mathbf{v}_i^T \quad \cdots \quad \mathbf{v}_{n+2}^T\right]^T \in R^{3(n+3)\times1}, \quad (15)$$

$$\mathbf{K} = diag\left(\mathbf{K}_0, ..., \mathbf{K}_i, ..., \mathbf{K}_{n+2}\right) \in R^{3(n+3)\times3(n+3)}, \quad (16)$$

$$\mathbf{K}_i = diag\left(k_{p_i}, k_{q_i}, k_{r_i}\right) \in R^{3\times3}. \quad (17)$$

2.3 Eigenvalue analysis

Differential equations of motion should be obtained as [1]:

$$\mathbf{M}\ddot{\mathbf{v}} + \mathbf{K}\mathbf{v} = \mathbf{0} \in R^{3(n+3)\times1}, \quad (18)$$

which implies the eigenvalue problem in the following form:

$$\left(\mathbf{K} - \omega_r^2\mathbf{M}\right)\mathbf{u}_r = \mathbf{0}, \ \left(r = 1, ..., 3(n+3)\times1\right), \quad (19)$$

where $\mathbf{u}_r$ represents the eigenvector which corresponds to natural frequency ω_r. In order to obtain the natural frequencies and their corresponding eigenvectors under different boundary conditions, it is necessary to remove the columns and vectors of the matrices **M** and **K** which correspond to the restricted displacements.

In addition, the proposed model of a double-cracked beam can be adjusted for the analysis of beams with one crack, as well as for beams without cracks. In the case of beam with one crack it is necessary to put into the proposed algorithm that $\mathbf{v}_{n_1+n_2+1} \equiv \mathbf{v}_{n_1+n_2+2}$, as well as in the case of uncracked beam it holds that $\mathbf{v}_{n_1} \equiv \mathbf{v}_{n_1+1}$ and $\mathbf{v}_{n_1+n_2+1} \equiv \mathbf{v}_{n_1+n_2+2}$.

3. NUMERICAL EXAMPLES

3.1. Beam with one crack

Let's consider here the pinned-pinned (P-P) beam with one crack of the following characteristics: L=0.4 [m], b=h=0.01 [m], E=2.16·10^{11} [N/m^2], ρ=7650 [kg/m^3], a_1/h=0.5, L_1/L=0.5.

Results obtained by using the proposed approach, experiment [4], and FEM are given in Table 2. Note that the FEM results are obtained by using Ansys software, whereas 2628 elements of type Solid 185 were used. The results obtained by the proposed approach are very close to the results of the experiment [4] as well as to the FEM results obtained by using Ansys. However, it can be noticed that the relative error increases with increasing order of the required frequency. Thus in the case of the third frequency, the relative error between the results of the proposed approach and FEM is 2.31 [%].

Table 2: Comparison of the first three natural frequencies of the P-P beam with one crack

Methods	Natural frequencies [Hz]		
	f_1	f_2	f_3
This study (n=100)	140.18	602.24	1271.04
FEM	138.96 (0.88 %)	596.05 (1.04 %)	1242.3 (2.31 %)
Experiment [4]	139.2 (0.7 %)	593.0 (1.56 %)	-

If we take a closer look at Figure 2, which shows the first three mode shapes of considered beam, it can be seen that the crack is closed in the third mode shape. This is contrary to the main assumption of this paper, that the crack is open all the time of beam vibration. So this fact is a possible reason for a slightly larger deviation of the obtained results in the case of the third frequency.

At this point, it is interesting to comment the influence of the position of the crack on the deviation in the value of the frequencies of the uncracked beam. Figure 3 (a) - (d) shows the change of the first three frequencies of the beam in relation to the corresponding values of the uncracked beam at different positions of the crack, for the most commonly used boundary conditions. The depth of the crack (a_1/h) in all considered cases is equal to 0.5. Only in the case of the first frequency of C-F beam, with increasing distance of the crack L_1, the difference between the frequency of the cracked and uncracked beam decreases. In all other cases of beam boundary conditions, the dependence of the obtained frequencies on the distance of the crack L_1 has an oscillatory character. Also, under symmetrical boundary conditions (P-P, C-C, and F-F), the obtained diagrams are symmetrical with respect to the center of the beam.

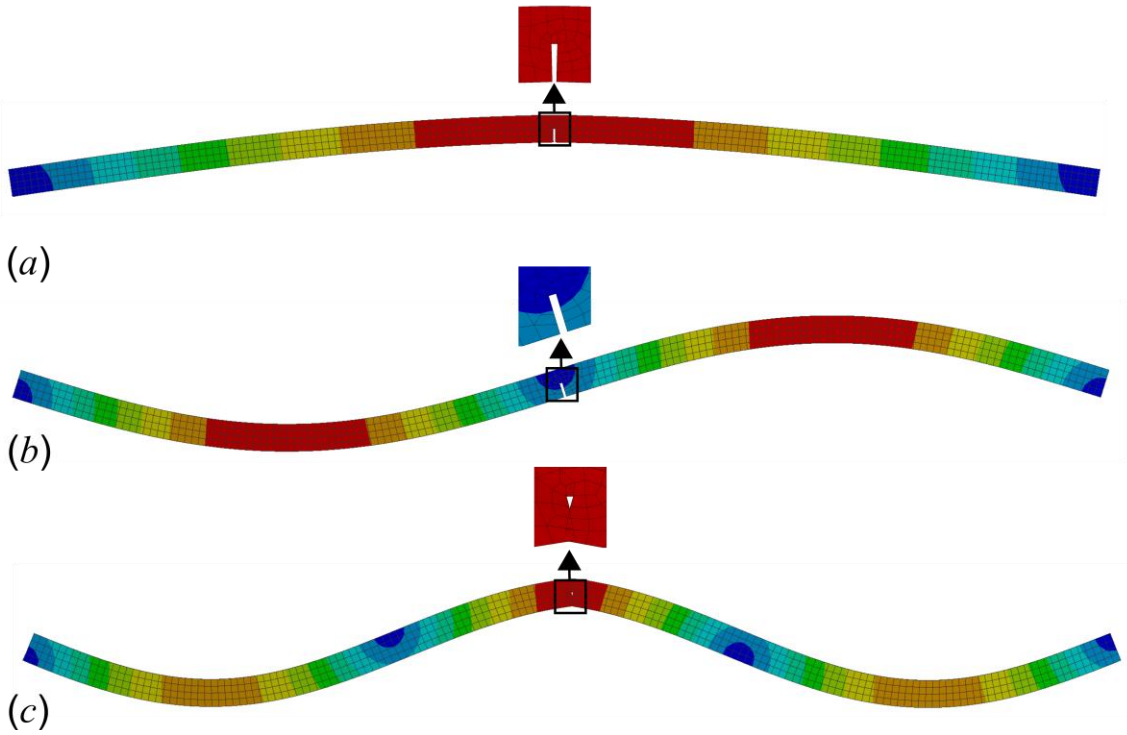

Figure 2: The first three mode shapes of the P-P beam with one crack

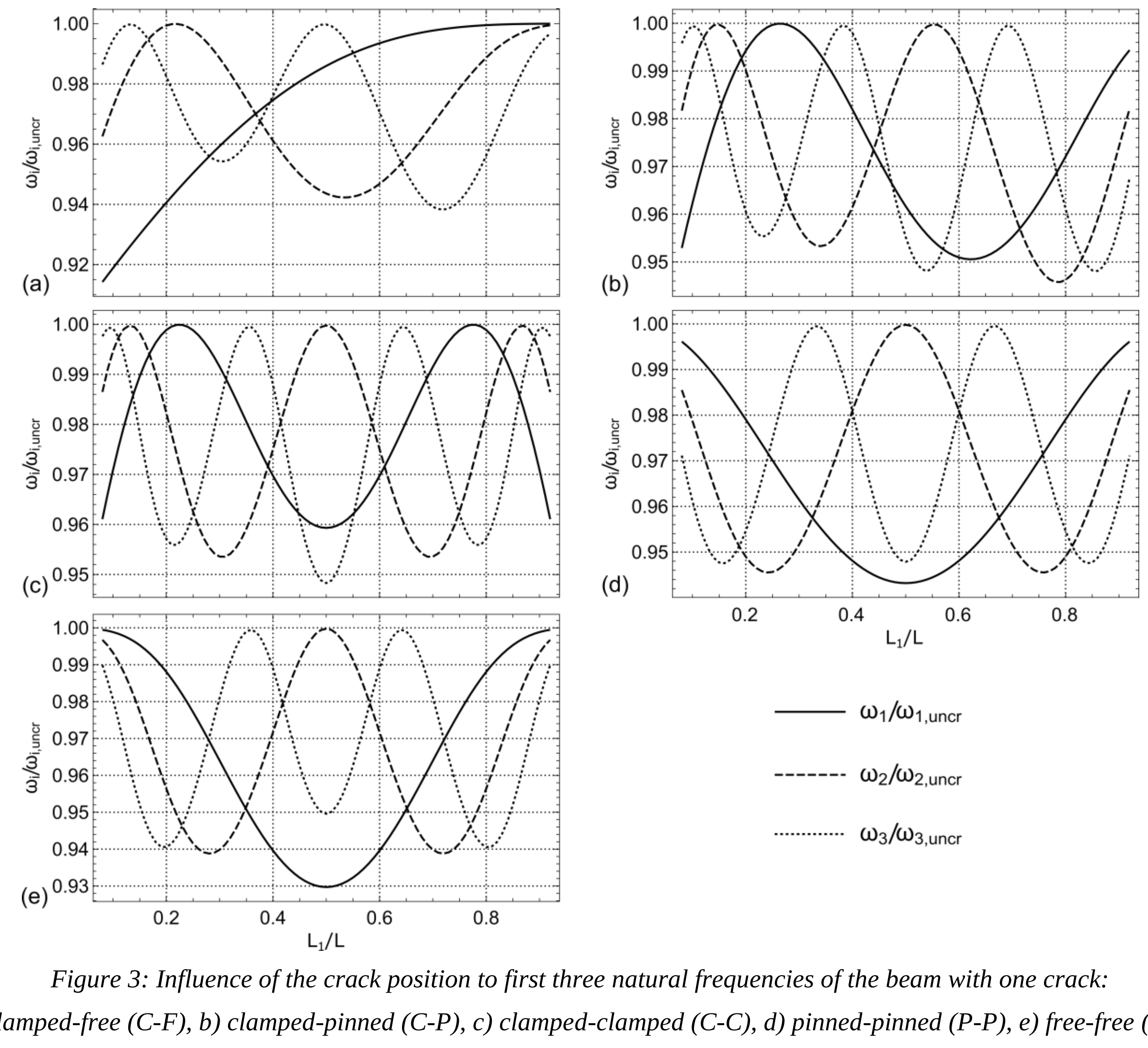

Figure 3: Influence of the crack position to first three natural frequencies of the beam with one crack: a) clamped-free (C-F), b) clamped-pinned (C-P), c) clamped-clamped (C-C), d) pinned-pinned (P-P), e) free-free (F-F).

3.2. Double-cracked beam

Here will be considered double-cracked beam with the cracks depth $a_1/h= a_2/h$ =0.5. The distances of the cracks from the left end are L_1/L=0.3 and L_2/L=0.7. All other beam parameters are the same as in the previous example. Table 2 shows the comparison of the results of this study and FEM at various boundary conditions.

The best results of this study are achieved in the C-F case, where the minimal error is equal to 1.01 % for the first frequency, and maximum error is in the case of third frequency and it is equal to 2.88 %. The worst results are in the case of P-P beam, where errors range from 2.48 % for the first frequency to 3.96 % for the third frequency. These are unexpectedly poor results compared to the previously achieved results of the rigid segment method [1] in the case of a single-cracked beam.

However, if we look at the first three mode shapes of the P-P double-cracked beam, obtained by using Ansys, then it can be seen that in the second mode shape the crack closes. It is obvious that the open crack model used here does not give sufficient accuracy in this case.

Table 2: Comparison of the first three natural frequencies of double-cracked beam at various boundary conditions

Boundary condition	Methods	Natural frequencies [Hz]		
		f_1	f_2	f_3
C-F	This study (n=100)	50.84 (1.01 %)	318.60 (1.10 %)	826.22 (2.88 %)
	FEM	50.33	315.14	803.09
C-P	This study (n=100)	223.21 (1.6 %)	692.87 (2.74 %)	1547.37 (2.31 %)
	FEM	219.7	674.35	1512.4
C-C	This study (n=100)	334.45 (0.02 %)	840.28 (2.35 %)	1774.87 (1.63 %)
	FEM	334.51	820.97	1746.4
P-P	This study (n=100)	137.96 (2.48 %)	535.22 (3.87 %)	1345.9 (3.96 %)
	FEM	134.62	515.26	1294.6
F-F	This study (n=100)	313.15 (1.87 %)	810.03 (3.34 %)	1762.32 (2.37 %)
	FEM	307.39	783.81	1721.6

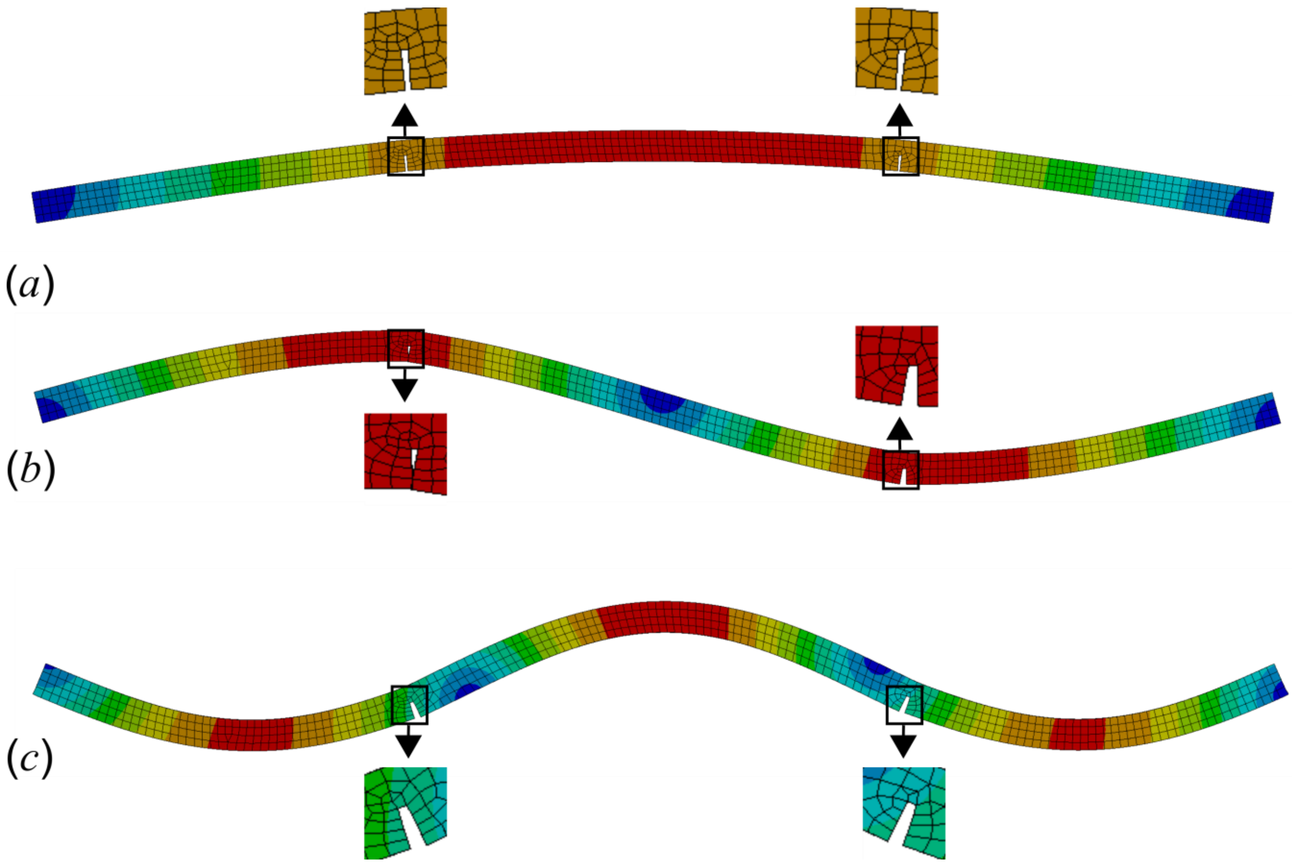

Figure 4: The first three mode shapes of P-P double-cracked beam

4. CONCLUSION

In this paper, the extension of the use of method of rigid segments to beams with two cracks is presented. Although at first glance it seems that the method will be just as effective in the case of the beam with two cracks, as it was the case with the beam with one crack, it is not so. It has been observed that a significantly larger error occurs when the crack closure is observed in one of vibration modes during vibration. Note only that the case where the depth of both cracks is equal to half of the cross-section height is analysed here. It is possible that at smaller crack depths this problem will be less pronounced. This would allow further use of this approach for the case of a beam with an arbitrary number of cracks, which will be the subject of further research by the author.

ACKNOWLEDGEMENTS

This research was supported under grant no. 451-03-9/2021-14/200108 by the Ministry of Education, Science and Technological Development of the Republic of Serbia. This support is gratefully acknowledged.

REFERENCES

[1] A. Nikolić and S. Šalinić, "Free vibration analysis of cracked beams by using rigid segment method", Appl. Math. Model., Vol. 84, pp. 158-172, (2020)

[2] D.Y.Zheng and N.J. Kessissoglou, "Free vibration analysis of a cracked beam by finite element method", J. Sound Vib., vol. 273(3), pp. 457-475, (2004)

[3] J. Banerjee, S. Guo, "On the dynamics of a cracked beam", Proceedings of the Fiftieth AIAA/ASME/ASCE /AHS/ASC Structural Dynamics and Materials, Palm Springs (California), 4–7 May 2009, pp. 1-11.

[4] H.I. Yoon, I.S. Son and S.J. Ahn, "Free vibration analysis of Euler-Bernoulli beam with double cracks", J. Mech. Sci. Technol., vol. 21(3), pp. 476-485, (2007)